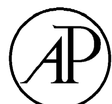

ACADEMIC PRESS

Journal of Solid State Chemistry 169 (2002) 19–23

JOURNAL OF SOLID STATE CHEMISTRY

www.academicpress.com

Electronic structure of β-Fe($Si_{2-x}Ge_x$) ternaries

Jun-ichi Tani* and Hiroyasu Kido

Department of Inorganic Chemistry, Osaka Municipal Technical Research Institute, 1-6-50 Morinomiya, Joto-ku, Osaka 536-8553, Japan

Received 11 April 2002; received in revised form 24 June 2002; accepted 5 August 2002

Abstract

The geometrical and electronic structures of β-Fe($Si_{2-x}Ge_x$) ternaries were investigated using first principles pseudopotential calculations based on generalized gradient approximation density function theory. These compounds are indirect-bandgap semiconductors with theoretical energy band gaps ranging from 0.51 to 0.79 eV. Substitution of Ge for Si in β-$FeSi_2$ leads to a reduction of the gap width and an increase in the volume of the unit cell with almost the same shape of the last valence band and the first conduction band but for the Y point. The analyses of bond overlap population and Mulliken population revealed that the covalency between Fe and Si atoms are strengthened by increasing Ge content and that the electron transfer occurs from Ge to Fe or Si.

© 2002 Elsevier Science (USA). All rights reserved.

Keywords: β-Fe($Si_{2-x}Ge_x$); Electronic structure calculations

1. Introduction

Transition metal silicides are of considerable interest in view of their structural and functional applications. The semiconducting phase of iron disilicide (β-$FeSi_2$) shown in Fig. 1 belongs to the *Cmca* space group (orthorhombic system) containing 48 atoms per unit cell (16 Fe atoms and 32 Si atoms). β-$FeSi_2$ has been studied as a material for optoelectronic and thermoelectric applications [1]. Many attempts have been made to dope additives into β-$FeSi_2$ to control its semiconducting properties. P-type conduction is found by doping with V, Cr, Mn, and Al doping, and n-type with Co, Ni, Pt, and Pd doping [2–9].

Requirements for thermoelectric materials include a large Seebeck coefficient S, a small electrical resistivity ρ, and a small thermal conductivity κ. These quantities determine the so-called thermoelectric figure of merit, $Z = S^2/\rho\kappa$. A low thermal conductivity and a high carrier mobility are desirable for an improved figure of merit. In other silicon-based materials such as Si and Mg_2Si, it is reported that Z is improved by the substitution of Si atoms with Ge in these materials [10,11]. For β-$FeSi_2$, the thermal conductivity might be decreased by replacement of Si by Ge because Ge has a larger radius and mass than Si. Moreover, theoretical models for the Z of narrow gap semiconductors predict the highest ZT at gap widths varying from 6 to 10 k_BT. According to the theoretical predictions, a narrower gap should lead to maximal ZT at lower temperatures, thereby altering the specifications of the thermoelectric device [12–14].

Recently, Chen et al. [15] reported a semiconducting Fe($Si_{2-x}Ge_x$) thin film grown on Si (100) by reactive deposition epitaxy using a high-vacuum evaporation technique. The direct band gap of $x = 0.08$ in Fe($Si_{2-x}Ge_x$) is determined to be 0.83 eV by optical transmission measurements, which indicate a redshift of the band gap with regard to that of β-$FeSi_2$ (E_g = 0.87 eV) thin films. However, to our knowledge, no theoretical data have been reported regarding the geometrical and electronic structure of Fe($Si_{2-x}Ge_x$).

In the present study, we performed for the first time the quantum-mechanical first principle calculations of the Fe($Si_{2-x}Ge_x$) ternary system within density functional theory. Although the solubility limit of Ge in β-$FeSi_2$ is unknown and orthorhombic heavily Ge doped β-$FeSi_2$ has not yet been synthesized because $FeGe_2$ belongs to the $I4/mcm$ space group (tetragonal system), the objective here is to explore the effects of the substitution of Ge in the Si in orthorhombic β-$FeSi_2$ on its geometrical and electronic structure.

*Corresponding author. Fax: +6-6963-8099.

E-mail addresses: tani@omtri.city.osaka.jp (J. Tani), kido@omtri.city.osaka.jp (H. Kido).

0022-4596/02/$ - see front matter © 2002 Elsevier Science (USA). All rights reserved.
PII: S0022-4596(02)00004-X

2. Details of the calculations

Density functional theory (DFT) calculations within the pseudopotential and generalized gradient approximations (GGAs) were performed using the computer program CASTEP (Cambridge Serial Total Energy Package in Cerius2, Accelrys Inc.) [16]. We constructed an orthorhombic β-$FeSi_2$ primitive unit cell of 24 atoms (4 Fe_I, 4 Fe_{II}, 8 Si_I, 8 Si_{II}) [17]. We replace the eight sites of the Si atoms by Ge partially or completely in this primitive unit cell. We expanded the valence electronic wave functions in a plane-wave basis set up to an energy cutoff of 560 eV, which converges the total energy of the unit cell to better than 1 meV/atom. In the total-energy calculations, integrations over the Brillouin zone were performed by using a $3 \times 3 \times 3$ Monkhurst-Pack set [18], which gives eight symmetrized k points. The electron–ion interaction is described by a norm-conserving potential generated using the optimization scheme of Lin et al. [19]. In the process of the calculation, the position of all atoms in the unit cell, as well as the lattice parameters, were allowed to relax by total energy minimization. At the optimized structure, the electronic structure was analyzed in terms of the atomic charges, bond overlap population, and band structures.

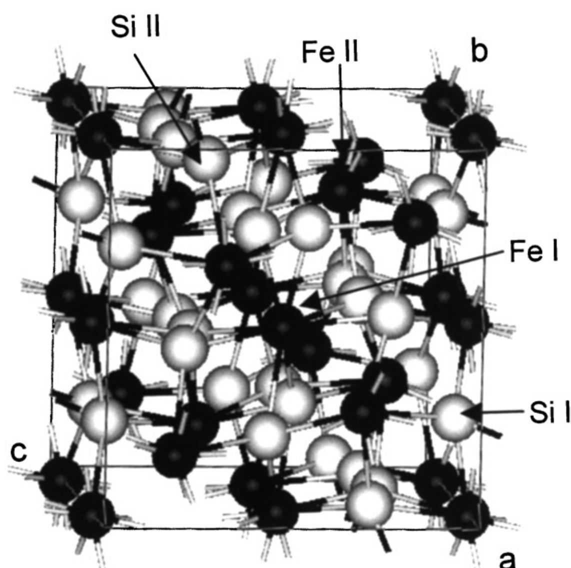

Fig. 1. Unit cell of β-$FeSi_2$. Black spheres represent Fe and white spheres represent Si. There are two crystallographically inequivalent sites of both Fe and Si (Fe_I, Fe_{II}, Si_I, Si_{II}).

3. Results and discussion

Table 1 shows the experimental and calculated structural parameters. FeGeSi and FeSiGe are that Ge atoms occupying all Si-1 and Si-2 sites in the β-$FeSi_2$ structure, respectively. The calculated values for $FeSi_2$ (relaxed structure) are in good agreement with the experimental results (unrelaxed structure) reported by Dusansoy et al. [20] within $\pm 0.02\%$. Lattice constants a–c increase with increasing Ge content. Lattice constants b, c of FeGeSi are almost the same values of those of FeSiGe, whereas lattice constant a of FeSiGe is larger than that of FeGeSi. The total energy calculation of FeGeSi is 7.5 meV per atom lower than that of FeSiGe. This calculation result predicts that Ge atoms preferably occupy the site Si_I.

Fig. 2 shows the Brillouin zone of the β-$FeSi_2$ structure based on the primitive unit cell. For each structure of β-$Fe(Si_{2-x}Ge_x)$ considered here, we have

Table 1
Calculated (relaxed) and experimental structural parameters (unrelaxed (Ref. [20]) for β-$FeXY$ (X, Y = Si or Ge) are given

Structural parameters	Experimental	Calculated			
	$FeSi_2$	$FeSi_2$	FeGeSi X = Ge, Y = Si	FeSiGe X = Si, Y = Ge	$FeGe_2$
a (Å)	9.863	9.8720	9.9468	9.9664	10.0603
b (Å)	7.791	7.7775	7.8201	7.8219	7.8643
c (Å)	7.833	7.8374	7.9090	7.9066	7.9888
Fe(a)$-x$	0.2146	0.2156	0.2157	0.2157	0.2162
Fe(a)$-y$	0.0	0.0	0.0	0.0	0.0
Fe(a)$-z$	0.0	0.0	0.0	0.0	0.0
Fe(b)$-x$	0.5	0.5	0.5	0.5	0.5
Fe(b)$-y$	0.3086	0.3080	0.3077	0.3078	0.3081
Fe(b)$-z$	0.1851	0.1852	0.1840	0.1845	0.1839
X(a) $- x$	0.1282	0.1283	0.1282	0.1280	0.1278
X(a) $- y$	0.2746	0.2743	0.2747	0.2737	0.2741
X(a) $- z$	0.0516	0.0515	0.0519	0.0499	0.0497
Y(b) $- x$	0.3727	0.3732	0.3731	0.3733	0.3731
Y(b) $- y$	0.0450	0.0455	0.0445	0.0453	0.0444
Y(b) $- z$	0.2261	0.2264	0.2276	0.2267	0.2281

calculated the electronic band structure along the lines indicated in Fig. 2.

Fig. 3 shows the band structure of the fully relaxed bulk structure of $FeSi_2$, FeGeSi, FeSiGe, and $FeGe_2$ along several lines of high symmetry. The valence band maximum exists at the Y point. Energy is measured relative to the Fermi level $E_F = 0$ eV. The calculated values of direct band gap, Δ, at the points Γ, Y, and Λ as well as the indirect band gap are listed in Table 2. The primitive cell of β-$FeSi_2$ exhibited an indirect band gap of 0.79 eV between the Y point in the valence band and the Λ point located at the $2/5(Z\Gamma)$ line in the conduction band, agreeing with the calculations of Miglio et al. [21] and Clark et al. [22]. This band gap value is in fairly good agreement with the experimental one of 0.83–0.89 eV [23]. The band gap of FeSiGe exhibited an indirect band gap of 0.65 eV between the Y point in the valence band and the Λ point in the conduction band which is smaller than that of FeGeSi, 0.67 eV. The primitive cell of $FeGe_2$ exhibited an indirect band gap of 0.51 eV between the Y point in the valence band and the point located at the $1/3(\Gamma S)$ line in the conduction band. The shape of the last valence band is close to that of β-$FeSi_2$, but for the Y point. Though a bigger dispersion in the valence band is observed around the Y point with increasing Ge content, Ge doping seems not to strongly affect the shape of the last valence band and the first conduction band. However, Chen et al. [15] reported the direct band transition of a semiconducting $Fe(Si_{2-x}Ge_x)$ thin film grown on Si (100) by means of reactive deposition epitaxy using a high-vacuum evaporation technique. The direct band gap of $FeSi_{1.92}Ge_{0.08}$ is determined to be 0.83 eV by optical transmission measurements, which indicates a redshift of the band gap with regard to that of β-$FeSi_2$ ($E_g =$ 0.87 eV) thin films. The calculated band gap of β-$FeSi_{2-x}Ge_x$ in our present work decreases with increasing Ge concentration (x). This tendency agrees well with the experimental results. The band gap can be controlled by the amount of Ge doping. Previous works by several authors have shown that the band gap in β-$FeSi_2$ is highly sensitive to its lattice parameters and the way they are grown (bulk or thin films). Therefore, the reason for decrease of band gap by Ge doping is considered to be not only simply due to the change of atomic species, but also due to the change of lattice parameters. Miglio and Meregalli [21] and Clark et al. [22] reported that the band structure in the Y point is strongly affected by the lattice constant of β-$FeSi_2$. It is reported that the effect of the strain of the lattice affects the transition route, that is, determines an indirect or direct route. This inconsistency between our calculation results and Chen et al. may be accounted for by the $Fe(Si_{2-x}Ge_x)$ thin film having the strain of the lattice, which affects the band structure.

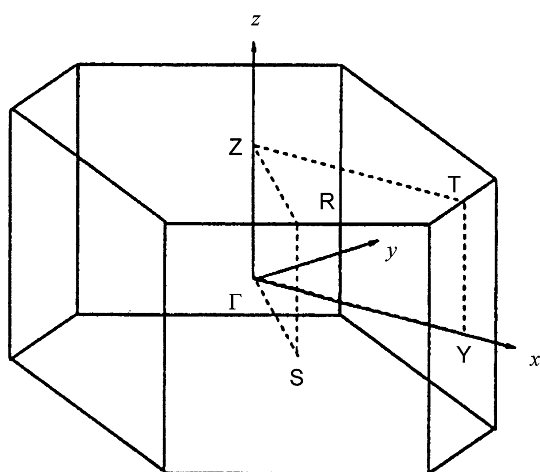

Fig. 2. The Brillouin zone of the β-$FeSi_2$ structure based on the primitive unit cell showing the lines along which the band structures shown in Fig. 3 were calculated.

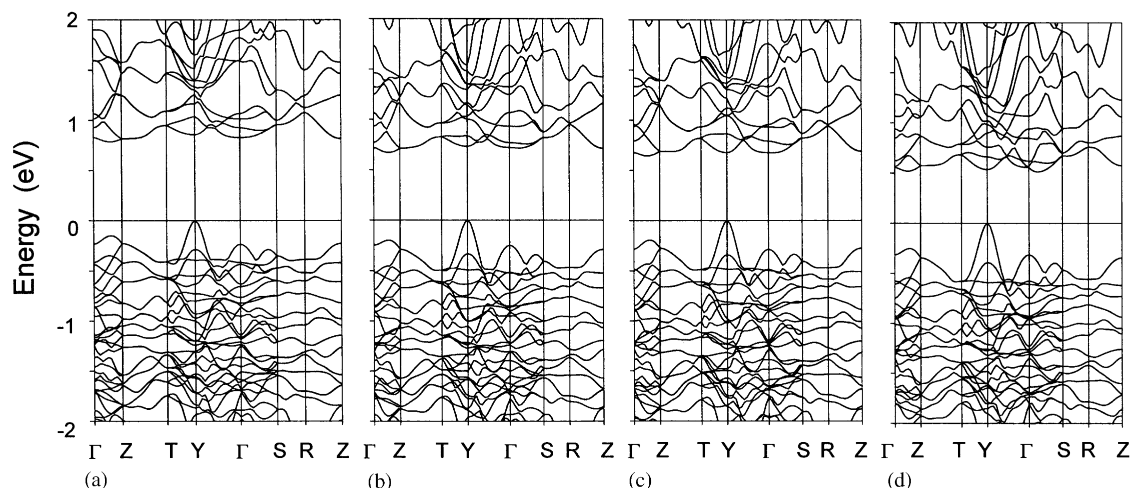

Fig. 3. Calculated band structure of (a) $FeSi_2$; (b) FeGeSi; (c) FeSiGe; and (d) $FeGe_2$ along several lines of high symmetry.

Table 3 shows the results of the Mulliken population analysis. In the unrelaxed $FeSi_2$, both the Fe_I and Fe_{II} show a small negative value of -0.02, whereas the Si_I show a small positive value of $+0.02$. In the relaxed $FeSi_2$, the Fe_I and Si_I show a small positive value of $+0.01$ and Si_{II} a small negative value of -0.01. This result suggests that the charges of Fe and Si depend not only on the sites (Fe_I, Fe_{II}, Si_I and Si_{II}), but also on the degree of the internal stress of individual atoms. The lattice and internal relaxation is found to have some effects on the results of the Mulliken population analysis. However, this calculation result clearly suggests that a large charge transfer from Fe to Si or from Si to Fe does not occur in $FeSi_2$.

However, in FeGeSi, FeSiGe, and $FeGe_2$ systems, Ge is positively charged in the range $+0.28$ and $+0.75$, whereas Fe_I and Fe_{II} are negatively charged in the range -0.53 and -0.67. Si_{II} for FeGeSi indicates a negative value, -0.12, and Si_I for FeSiGe indicates a negative value, -0.09. These results clearly suggest that electron transfer occurs from Ge to Fe or Si by replacing Ge on the Si site.

The characteristics of this electronic interaction can be studied by means of the bond overlap population analysis. Table 4 shows the average value of the bond distance and bond overlap population between Fe and X (X = Si or Ge atoms), which is the average value between Fe and X atoms located at the FeX_8 octahedra unit. In $FeSi_2$, the average value of the bond overlap population of Fe_I–Si indicates 0.17, which is slightly larger than that of Fe_{II}–Si, 0.15. The difference between the absolute values of the bond overlap population at Fe_I–Si and Fe_{II}–Si may be simply due to the difference between the lengths of the Fe_I–Si and Fe_{II}–Si bonds. The average length of the Fe_I–Si bond is 0.2359 nm, which is slightly shorter than that of the Fe_{II}–Si bond, 0.2381 nm. The average lengths of the Fe_I–Si bond and Fe_{II}–Si bond for FeGeSi and FeSiGe are 0.2368–0.2408 nm, which are slightly longer than that for $FeSi_2$. However, the bond overlap populations of Fe_I–Si and Fe_{II}–Si for FeGeSi and FeSiGe indicate 0.36–0.45, which are larger than that for $FeSi_2$. The covalency of Fe–Si is also strengthened by increasing the Ge content. The average overlap populations between the Fe_{II}–Ge atoms for FeGeSi and FeSiGe indicate -0.02–0.43. In $FeGe_2$, the average value of the bond overlap population for Fe_I–Ge indicates 0.61, which is larger than that of Fe_{II}–Ge, 0.38. The bond overlap populations of Fe_I–Ge as well as Fe_{II}–Ge for $FeGe_2$ are much larger than those of Fe_I–Si as well as Fe_{II}–Si for $FeSi_2$, which strongly suggests that the covalency of Fe–Ge is stronger than that of Fe–Si.

Table 2
Direct band gap, Δ, at the points Γ, Y, and Λ as well as the indirect band gaps $\Delta_{indirect}$ with the direction in reciprocal space given in parentheses

Compound	Δ			$\Delta_{indirect}$
	Γ	Y (eV)	Λ	(eV)
$FeSi_2$	1.06	0.86	0.93	0.79 ($Y \to \Lambda$)
FeGeSi	0.97	0.73	0.97	0.67 ($Y \to \Lambda$)
FeSiGe	0.97	0.68	0.84	0.65 ($Y \to \Lambda$)
$FeGe_2$	0.83	0.54	0.77	0.51 ($Y \to \Gamma$–S)

Table 3
Electronic charges (in e) of the atoms in β-$FeSi_{2-x}Ge_x$ obtained by Mulliken population analysis

Samples	Fe_I	Fe_{II}	Si_I	Si_{II}	Ge_I	Ge_{II}
$FeSi_2$ (unrelaxed)	−0.02	−0.02	+0.02	0.00		
$FeSi_2$ (relaxed)	+0.01	0.00	+0.01	−0.01		
FeGeSi	−0.67	−0.59		−0.12	+0.75	
FeSiGe	−0.67	−0.59	−0.09			+0.72
$FeGe_2$	−0.66	−0.53			+0.28	+0.31

4. Conclusion

The geometrical and electronic structures of β-$Fe(Si_{2-x}Ge_x)$ ternaries were investigated using first principles pseudopotential calculations based on generalized gradient approximation density function

Table 4
Distances (r) and bond overlap populations between Fe atoms and Si or Ge, which are the average value between Fe and Si or Ge atoms located at FeX_8 (X = Si or Ge atoms)

Samples	Fe_I–Si		Fe_{II}–Si		Fe_I–Ge		Fe_{II}–Ge	
	r (nm)	Bond overlap population	r (nm)	Bond overlap population	r (nm)	Bond overlap population	r (nm)	Bond overlap population
$FeSi_2$	0.2359	0.17	0.2381	0.15				
FeGeSi	0.2383	0.45	0.2408	0.36	0.2369	0.43	0.2405	0.36
FeSiGe	0.2368	0.41	0.2405	0.44	0.2386	0.30	0.2394	−0.02
$FeGe_2$					0.2396	0.61	0.2420	0.38

theory. These compounds are indirect-bandgap semiconductors with theoretical energy band gaps ranging from 0.51 to 0.79 eV. Substitution of Ge for Si in β-$FeSi_2$ leads to a reduction of the gap width and an increase in the volume of the unit cell with almost the same shape of the last valence band and the first conduction band, but for the Y point. The analyses of bond overlap population and Mulliken population revealed that the covalency between Fe and Si atoms is strengthened by increasing the Ge content and that the electron transfer occurs from Ge to Fe or Si.

References

[1] D.M. Rowe, CRC Handbook of Thermoelectrics, CRC Press, New York, 1995, p. 287.
[2] R.M. Ware, D.J. McNeill, Proc. IEE 111 (1964) 178.
[3] U. Birkholz, J. Schelm, Phys. Status Solidi 27 (1968) 413.
[4] I. Nishida, Phys. Rev. B 7 (1973) 2710.
[5] T. Kojima, Phys. Status Solidi A 111 (1989) 233.
[6] M. Komabayashi, K. Hijikata, S. Ido, Jpn. J. Appl. Phys. 30 (1991) 331.
[7] J. Tani, H. Kido, J. Appl. Phys. 84 (1998) 1408.
[8] J. Tani, H. Kido, J. Appl. Phys. 86 (1999) 464.
[9] J. Tani, H. Kido, Jpn. J. Appl. Phys, 38 1999 (2717).
[10] G.A. Slack, M.A. Hussain, J. Appl. Phys. 70 (1991) 2694 and references therein.
[11] Y. Noda, H. Kon, Y. Furukawa, N. Otsuka, I. A. Nishida, K. Masumoto, Mater. Trans. JIM 33 (1992) 845.
[12] R.P. Chasmar, R. Stratton, J. Electron. Control 7 (1959) 52.
[13] G.D. Mahan, J. Appl. Phys. 65 (1989) 1578.
[14] J.O. Sofa, G.D. Mahan, Phys. Rev. B 49 (1994) 4565.
[15] H. Chen, P. Han, X.D. Huang, L.Q. Hu, Y. Shi, Y.D. Zheng, Appl. Phys. Lett. 69 (1996) 1912.
[16] CASTEP Users Guide, Accelrys Inc., San Diego, CA, 2001.
[17] A.B. Filonov, D.B. Migas, V.L. Shaposhnikov, N.N. Dorozhkin, G.V. Petrov, V.E. Borisenko, W. Henrion, H. Lange, J. Appl. Phys. 79 (1996) 7708.
[18] H.J. Monkhorst, J.D. Pack, Phys. Rev. B 13 (1976) 5188.
[19] J.S. Lin, A. Qteish, M.C. Payne, V. Heine, Phys. Rev. B 47 (1993) 4174.
[20] Y. Dusansoy, J. Protas, R. Wandij, B. Roques, Acta Crystallogr. B 27 (1971) 1209.
[21] L. Miglio, V. Meregalli, J. Vac. Sci. Technol. B 16 (1998) 1604.
[22] S.J. Clark, H.M. Al-Allak, S. Brand, R.A. Abram, Phys. Rev. B 58 (1998) 10389.
[23] H. Lange, Phys. Status Solidi B 201 (1997) 3 and reference therein.